Scand J Med Sci Sports 2013: 23: e353–e360
doi: 10.1111/sms.12089

SCANDINAVIAN JOURNAL OF MEDICINE & SCIENCE IN SPORTS

Increased mast cell numbers in a calcaneal tendon overuse model

J. Pingel[1], J. Wienecke[2], M. Kongsgaard[1], H. Behzad[3], T. Abraham[4], H. Langberg[5], A. Scott[3]

[1]Institute of Sports Medicine, Department of Orthopaedic Surgery M. Bispebjerg Hospital and Center for Healthy Aging, Faculty of Health Sciences, University of Copenhagen, Copenhagen, Denmark, [2]Department of Neuroscience & Department of Exercise and Sport Sciences, Faculty of Health Sciences, University of Copenhagen, Copenhagen, Denmark, [3]Centre for Hip Health and Mobility, Vancouver Coastal Health Research Institute, Department of Physical Therapy, University of British Columbia, Vancouver, British Columbia, Canada, [4]James Hogg Research Centre, St Paul's Hospital, Vancouver, British Columbia, Canada, [5]CopenRehab and Institute Public Health, Department of Public Health and Centre for Healthy Ageing, Faculty of Health Sciences, University of Copenhagen, Copenhagen, Denmark
Corresponding author: Jessica Pingel, PhD, Institute for Sports Medicine, Bispebjerg Hospital, Copenhagen and Centre for Healthy Aging, Bispebjergbakke 23, Build. 8. 1st. Floor, 2400 Copenhagen NV, Denmark. Tel: +45 35315060, Fax: +45 35312733, E-mail: jessica.pingel@gmail.com

Accepted for publication 2 May 2013

Tendinopathy is often discovered late because the initial development of tendon pathology is asymptomatic. The aim of this study was to examine the potential role of mast cell involvement in early tendinopathy using a high-intensity uphill running (HIUR) exercise model. Twenty-four male Wistar rats were divided in two groups: running group ($n = 12$); sedentary control group ($n = 12$). The running-group was exposed to the HIUR exercise protocol for 7 weeks. The calcaneal tendons of both hind limbs were dissected. The right tendon was used for histologic analysis using Bonar score, immunohistochemistry, and second harmonic generation microscopy (SHGM). The left tendon was used for quantitative polymerase chain reaction (qPCR) analysis. An increased tendon cell density in the runners were observed compared to the controls ($P = 0.05$). Further, the intensity of immunostaining of protein kinase B, $P = 0.03$; 2.75 ± 0.54 vs 1.17 ± 0.53, was increased in the runners. The Bonar score ($P = 0.05$), and the number of mast cells ($P = 0.02$) were significantly higher in the runners compared to the controls. Furthermore, SHGM showed focal collagen disorganization in the runners, and reduced collagen density ($P = 0.03$). IL-3 mRNA levels were correlated with mast cell number in sedentary animals. The qPCR analysis showed no significant differences between the groups in the other analyzed targets. The current study demonstrates that 7-week HIUR causes structural changes in the calcaneal tendon, and further that these changes are associated with an increased mast cell density.

Tendinopathy is a highly prevalent musculo-skeletal pain syndrome defined by the presence of tendon pain and thickening. Like osteoarthritis, the onset of overuse tendinopathy is typically insidious and associated with a history of increased mechanical loading (Maffulli et al., 2003). There has been a largely successful, although controversial, movement to abandon use of the term "tendinitis" for symptoms that last longer than 3 months, in recognition of the need to address degenerative structural changes within the tendon (i.e., tendinosis) rather than inflammation, which is argued to be rarely or only minimally present in later stages (Khan et al., 2002; Abate et al., 2009).

The cell populations present in tendons displaying features of tendinopathy were recently reinvestigated using tissue-specific immunolabeling for macrophages, lymphocytes, endothelial cells, smooth muscle cells, and mast cells (Scott et al., 2008). Compared with control tissue, the tendons from patients with a diagnosed, activity-related tendon disorder (patellar tendinopathy) demonstrated a substantially increased presence of neurovascular tissue and accompanying mast cells, compared with tendon from symptom-free patients. This study led the authors' attention toward the possibility that mast cells, and potentially a neurogenic inflammatory response, may be playing a hitherto unrecognized role in tendon overuse injuries. A recent study furthermore found increased numbers of mast cells and macrophages in early/mild or moderate rotator cuff tendinopathy (Millar et al., 2010).

In a subsequent acute tendon injury model, it was observed that the local mast cell density increases following tendon trauma (Sharma et al., 2011). Strikingly, mice injected with a mast cell inhibitor (sodium cromolyn) experienced less tendon thickening, reduced evidence of TGF-beta-related gene expression, and less tenocyte proliferation compared with controls. This injury model duplicated certain features of human pathology particularly at later time points (e.g., collagen disarray, increased mast cell density, vascular

Table 1. Running protocol

Week	Training	Warm-up	Warm-up	Exercise velocity	Exercise duration	Inclination
		Velocity (m/min)	Duration (min)	Velocity (m/min)	Duration (min)	%
1	1	10	5	15	30	8
1	2	10	5	16	45	8
1	3	10	5	17	60	8
1	4	10	5	18	60	8
2	5	10	5	19	60	8
2	6	10	5	20	60	8
2	7	10	5	20	70	8
2	8	10	5	21	70	8
3	9	10	5	21	80	8
3	10	10	5	22	80	8
3	11	10	5	22	90	8
3	12	10	5	23	90	8
4	13	10	5	23	100	8
4	14	10	5	24	100	8
4	15	10	5	24	100	8
4	16	10	5	25	100	8
5	17	10	5	25	100	8
5	18	10	5	26	100	8
5	19	10	5	26	100	8
5	20	10	5	27	100	8
6	21	10	5	27	100	8
6	22	10	5	28	100	8
6	23	10	5	28	100	8
6	24	10	5	29	100	8
7	25	10	5	29	100	8
7	26	10	5	30	100	8
7	27	10	5	30	100	8
7	28	10	5	30	100	8

Table 2. Weight development of the rats (g)

	1 week	2 weeks	3 weeks	4 weeks	5 weeks	6 weeks	7 weeks
Running	194	226	285	328	359	379	402
Control	195	232	297	351	391	425	459

hyperplasia, increased glycosaminoglycan). However, the potential influence of cyclic mechanical loading on the density of mast cells in tendon tissue has not yet been addressed. Mechanical loading is known to induce tenocytes to produce a variety of inflammatory cytokines including PGE2 and substance P (SP), which could directly or indirectly influence the behavior of mast cells (Feng et al., 2006; Theoharides et al., 2012).

The main hypotheses of the current study were that, compared to control (sedentary) rats, an intensive treadmill running program would lead both to an increased density of mast cells, and to features consistent with the development of early tendinopathy including (a) increased Bonar histopathologic score, (b) increased tendon cell density, (c) increased tendon protein kinase B (PKB) levels, and (d) decreased collagen organization.

Materials and methods

Training protocol

Twenty-four male Wistar Rats ($n = 12$ running rats, and $n = 12$ control rats; aged 7 weeks; mean weight 194 ± 9 g) were used for this study. This study was approved by the Regional Ethics Committee for animal experiments and adhered to the institutional guidelines for the care and treatment of laboratory animals (2009/561-1743). The animals were housed two per cage at 21 °C in a 12:12-h light-dark cycle and given food and water *ad libitum*. The running exercise were done in the morning, and the duration of the running protocol was four times a week for 7 weeks, over the course of which running velocity and intensity were gradually increased, ending with 100 min uphill running (8% inclination) with a running speed of (30 m/min) (Table 1). The control rats did not do any kind of exercise but were allowed normal cage activity. The development of weight changes of the rats over time is shown in Table 2.

Tissue preparation

In both protocols, the rats were euthanized with 2% isoflurane (Baxter A/S, Allerød, Denmark) and then decapitated. Both calcaneal tendons of the hindlimbs were immediately dissected. The left calcaneal tendon was snap frozen in liquid nitrogen for RNA extraction, and the right calcaneal tendon was removed with a piece of muscle still attached, longitudinally oriented in cryoprotectant medium [OCT Tissue Tek®, Sakura Finetek, Alphen aan den Rijn, the Netherlands (polyvinylalcohol <11%; carbowax <5%; nonreactive ingredients >85%)] and frozen in isopentane

chilled in liquid nitrogen for immunohistochemical and histological analysis. After collection, samples were stored in a –80 freezer until further analysis and transported between laboratories on dry ice. After cutting a number of cryosections for immunohistochemistry, the remainder of the tendon tissue was thawed and fixed in 4% paraformaldehyde in phosphate buffered saline and embedded in paraffin for morphological analysis.

Histology, immunohistochemistry

Protein kinase B immunohistochemistry was performed using a rabbit polyclonal antibody (Cell Signaling 4685; Cell Signaling Technology, Beverly, Massachusetts, USA) at 1:25 dilution, incubated at room temperature for 2 h. Antigen retrieval was performed with sodium citrate on the Ventana Discovery XT, and detection was with UltraMap DAB anti-rabbit (Ventana Medical Systems Inc, Tucson Arizona, USA). Paraffin blocks were sectioned at 5 microns thickness, and stained with hematoxylin and eosin or Alcian Blue pH <2.5. A single slide was prepared for each tendon.

Quantitative image analysis of micrographs

All histological analysis was conducted on de-identified, randomized slides, each comprising a single tissue section. Total tissue section area (mm^2) was determined by scanning each slide using a calibrated digital slide scanner, 20× objective (ScanScope XT, Aperio Technologies, Vista, California, USA). Tendon cell density was assessed by capturing the three most centrally located fields containing only tendon cells (i.e., cells embedded within the tendon proper collagen matrix, not including paratendon or insertional regions and avoiding vessels), using a 20× objective (microscope: Eclipse E600, Nikon Instruments, Melville, New York, USA; digital camera: SPOT Flex, Diagnostic Instruments, Sterling Heights, Michigan, USA), and calculating the average number of nuclei per viewing field. For individual tendon sections, the standard error of the mean (SEM) ranged from 0.88 to 22.8, with the average SEM being 8.0 in control rats and 10.0 in running rats. Because there is as yet no validated tenocyte marker for rat histological sections that we are aware of, we operationally defined tendon cells as fibroblast-like cells embedded within the tendon proper (i.e., avoiding the paratendon and entheseal regions and vessels). Mast cell density was determined by counting all mast cells identified on Alcian Blue-stained slides (containing brightly stained blue cytoplasmic granules) on the entire tissue section, including both tendon and paratendon, and normalizing to total tissue area. The intensity of PKB immunoreaction for control and sedentary rats was determined by scanning each slide using a calibrated digital slide scanner, 20× objective (ScanScope XT), and using automated thresholding (ScanScope software, v.9.1) to identify all non-artifactual stained pixels in the tissue section (hue value 1.0, hue width 0.73, saturation threshold 0.1).

Semiquantitative histological evaluation

Tendon was assessed using a previously validated scale which assigns a value to degenerative features commonly seen in chronic human tendinosis lesions (the modified Bonar score). Using the same systematically captured, de-identified digital images used for the calculation of tendon cell density, the extent of changes were assessed by a single examiner. The assessor assigned a score of 0–3 for each of five categories; tenocyte morphology, tenocyte proliferation, collagen organization, GAGs, and neovascularization. Using this scale, a completely normal tendon would score 0, whereas a tendon with the maximum score in all categories would score 15. In other words, the scores for each category were totaled (not averaged). The Spearman's correlation coefficient (R^2) for test-retest reliability on mechanically loaded rodent tendon was previously found to be 0.81 (Scott et al., 2007).

SHG/multiphoton excitation fluorescence analysis

Collagen structures in the same 24 histological specimens (one slide per tendon, one tissue section per slide) described above were visualized using second harmonic generation (SHG) microscopy. The three most centrally located fields containing only tendon cells (i.e., cells embedded within the tendon proper collagen matrix, not including paratendon or insertional regions and avoiding vessels), were assessed. The method used was exactly as previously described, generating an index of the density of organized (fibrillar) collagen. The total SHG signal intensity values in the forward direction were determined by systematically scanning each tissue section using the 20× objective and normalizing the obtained values to the cropped collagen area (μm^2). This technique exploits the property of collagen that, when stimulated with two photons separated by a wavelength of 440 nm, a fluorescent signal arising specifically from fibrillar collagen is generated. The strength of this signal is directly related to the density of the collagen fibrils.

RNA isolation

Total RNA was extracted from tendon tissue using a modification of TRIspin method. Briefly, frozen tendons were powdered in a tissue mill (Mikrodismembrator S, Sartorius, Göttingen, Germany) for 30 s at 16 200 *g* in liquid nitrogen cooled cryogenic tubes (Nalgene, Penfield, New York, USA). Trizol (1 mL) was added to the powdered tissue and the samples were rocked on a Vari Mix Platform Rocker (Fisher Scientific, Hamptom, New Hampshire, USA) for 10 min at room temperature after which chloroform (0.2 mL/1 mL TRIzol) was added, the samples were mixed vigorously, and centrifuged at 16 200 *g* for 15 min at 4 °C. The aqueous phase was removed and one volume of 70% ethanol was added to the aqueous phase. Total RNA was isolated from this mixture using RNeasy Mini Kit (QIAGEN, Gaithersburg, Maryland, USA) following the manufacturer's protocol. The RNA concentration in each sample was measured using the Nanodrop 2000 Spectrophotometer (Thermo Scientific, Hamptom, New Hampshire, USA).

Reverse transcription and qPCR

Total RNA was reverse transcribed to cDNA using the High Capacity cDNA Reverse Transcription Kit (Applied Biosystems, Foster City, California, USA) according to the manufacturer's instruction. Quantitative reverse transcription polymerase chain reaction (RT-PCR) was performed using the FastStart Universal SYBR Master Mix (Roche Applied Science, Indianapolis, Indiana, USA), and the Applied Biosystems 7500 Fast Real-Time PCR System. The data was analyzed using the comparative Ct method (Schmittgen & Livak, 2008). The relative abundance of the gene transcript was calculated as ΔCt ($\Delta Ct = Ct^{Reference} - Ct^{Target}$). Relative changes in transcript were expressed as ΔΔCt ($\Delta\Delta Ct = \Delta CT^{Runners} - \Delta Ct^{Sedentary}$). GAPDH was used as the reference gene to normalize target gene expression. The mRNA sequences of the reference and target genes were obtained from NCBI database. Primers were designed using the Primer 3 software (Whitehead Institute for Biomedical Research, Cambridge, Massachusetts, USA) and checked using Primer-Blast (NCBI database). All the primers were purchased from Invitrogen (Carlsbad, California, USA) and are listed in Table 3.

Statistical analysis

To compare the Bonar scale, SHG signal normalized to collagen area, and PKB intensity in the calcaneal tendons of sedentary and running rats, unpaired *t*-tests were used. For qPCR analysis, the data were inspected and an unpaired *t*-test was conducted for the relative quantity of IL-3, followed by Pearson's correlation coefficient to examine the relationship between IL-3 mRNA levels and mast cell density. Tests were conducted using online statistical calculators developed by Vassar College. The level of significance (alpha) was 0.05.

Table 3. Primers used for real-time qPCR

Gene symbol	Forward and reverse primers
GAPDH	Forward__5′ GGGCTCTCTGCTCCTCCCTGT3′ Reverse_5′ACGGCCAAATCCGTTCACACC3′
Tpsab1	Forward_5′CCTCCAACCGGGCCCGTACT3′ Reverse_5′TAGCTAGACTAGGGGCTGCGTGC3′
Tpsb2	Forward_5′GCCGAGACAGCCAAGATGCT3′ Reverse_5′CGCGTGCACCAGACTAGCCA3′
IL-6	Forward_5′TCTCGAGCCCACCAGGAACGA3′ Reverse_5′ACTGGCTGGAAGTCTCTTGCGGA3′
IL-3	Forward_5′GCGACTCTGTGTTGCCAGGTGT3′ Reverse_5′ACTGACACTGGCTGCAGGTCCTT3′
IL-1b	Forward_5′CCCTGCAGCTGGAGAGTGTGG3′ Reverse_5′ACCAGTTGGGGAACTGTGCAGAC3′
SCF	Forward_5′GCAGTAGCAGTAATAGGAAAGCCGC3′ Reverse_5′ATGAGAGCCGGCAGTGCCAT3′
NK1R	Forward_5′AACGACAGGTTCCGTCTGGGC3′ Reverse_5′TCTCCAGGCGGCTGACCTTGT3′
c-kit	Forward_5′ATCCTCCTCACTCACGGGCGG3′ Reverse_5′ACGGGCAGCCGTGCATTTCC3′

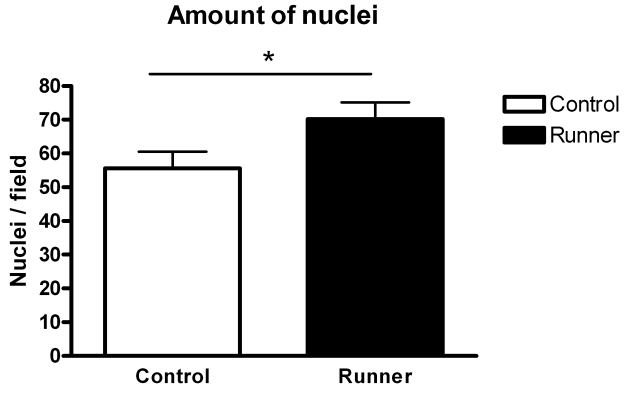

Fig. 1. Tenocyte proliferation, amount of nuclei, data shown in mean ± SEM (*level of significance $P \leq 0.05$).

Results

All rats were able to successfully complete the treadmill running protocol (Table 1). Running rats continued a trend of healthy weight gain throughout the study (Table 2). No rat demonstrated macroscopic signs of injury or behavioral symptoms of distress during the study.

Tendon cell proliferation and PKB intensity

In the current study, the density of tendon cells was increased in the calcaneal tendon of rats which had been subjected to the 7-week overuse protocol (Fig. 1). There was no difference overall in the area of PKB staining in the two groups; however, the total intensity of staining (indicative of PKB expression level) was significantly increased [average intensity of positive pixels, 6.56×10^9 (1.92×10^9) vs 4.39×10^9 (2.88×10^9), $P = 0.03$].

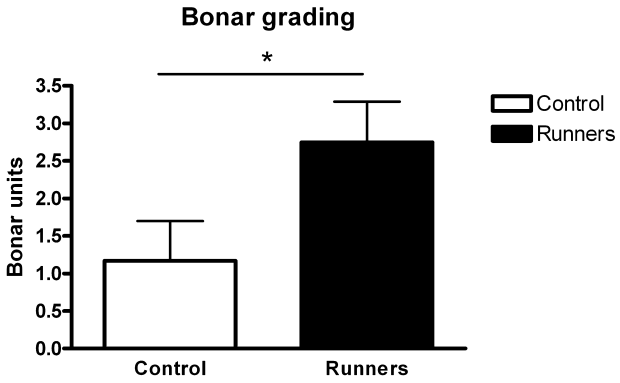

Fig. 2. Bonar grading, data shown in mean ± SEM (*level of significance $P \leq 0.05$).

Tendon degeneration

The presence of structural change was confirmed by the Bonar grading of the same areas, which demonstrated a significantly increased Bonar score in the animals which had run for 7 weeks (Fig. 2). The observed features were tenocyte abnormality (rounding and, in one runner's calcaneal tendon, chondroid change), increased cellularity, and loss of collagen organization; with the exception of chondroid change, these features were noted in both groups, but were of a more advanced nature (i.e., receiving a higher grade: running group 2.75 ± 0.54; control group 1.17 ± 0.53) in the running rats. Increased vascularity was not observed in either group. There was an appearance of expanded vascular paratendon in the runners, but this feature is not assessed in the Bonar grading.

Collagen organization

In control rats, the SHG signal intensity, normalized to collagen area, was 882 (23.8) AU, which was significantly higher than the signal arising from running rats, 793.5 (24.6) AU ($P = 0.03$). Areas of collagen disorganization were highly focal and localized to the tendon midsubstance (Fig. 3).

Mast cell density

When examining the Alcian Blue-stained slides, a substantial number of mast cells were observed in the paratendinous tissue. These cells were quantitated, normalized to total tissue section area, and compared in runners vs control animals. There were approximately three times as many mast cells in the calcaneal tendon tissue from running animals tissue [running group: 9.05 ± 1.95 (mast cells/mm^2); control group: 2.85 ± 1.31 (mast cells/mm^2), $P = 0.02$] (Fig. 4). The overall density and distribution of mast cells was similar to that observed in human patellar tendon (Scott et al., 2008).

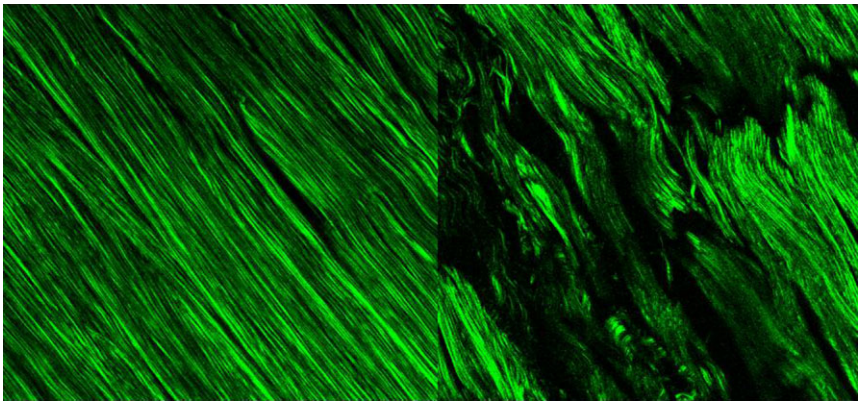

Fig. 3. Second harmonic generation images of collagen disorganization of rat calcaneal tendon. Left: sedentary rat; right: running rat (20× objective).

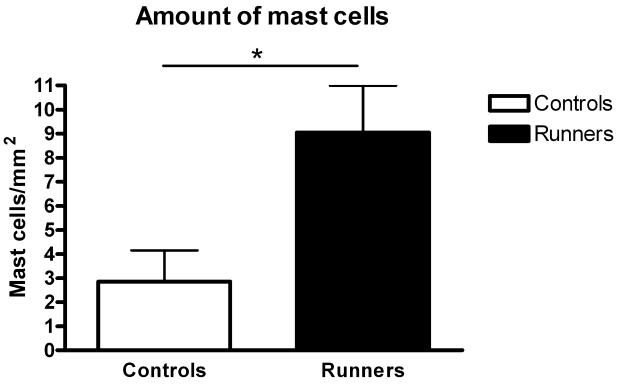

Fig. 4. Density of mast cells, data shown in mean ± SEM (*level of significance $P \leq 0.05$).

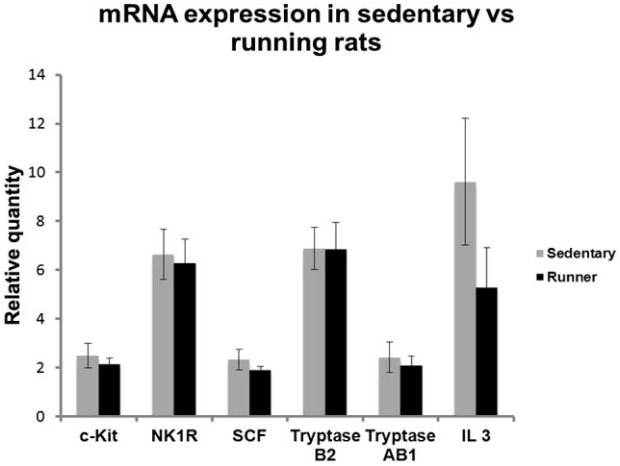

Fig. 5. mRNA expression in sedentary vs running rats, data shown in mean ± SD (*level of significance $P \leq 0.05$).

qPCR analysis

Because we observed an increased calcaneal tendon mast cell density in rats, which had been running, we analyzed several mast cell-related genes including: c-kit, NKIR, SCF, Tryptase B2, Tryptase AB1, and IL-3 in the tendon tissue samples obtained from runners and controls (Fig. 5). None of the genes showed any significant changes between the two groups when normalized to the housekeeping gene. Although IL-3 was not statistically different between groups ($P = 0.10$), we observed that mast cell density was significantly correlated to IL-3 levels in sedentary animals ($r^2 = 0.49$, $P = 0.04$) but not in runners ($r^2 = 0.06$).

Discussion

The current study adds to the growing body of evidence pertaining to the potential importance of mast cells in the development of overuse tendinopathy, documenting a substantial increase in mast cells in the calcaneal tendons of rats subjected to a 7 weeks, intensive running model. Mast cells produce and release substantial quantities of substances, which contribute to tissue repair and fibrosis, including TGF-beta, mast cell tryptase, and VEGF. Taken in the context of previous studies, which have shown an impact of mast cell inhibitors of post-injury tendon remodeling (Sharma et al., 2011), it is likely that the increased number of mast cells observed in the current study plays a role in the development or progression of overuse tendinopathy.

The completely novel finding that the density of mast cells in chronically painful human tendon is abnormally high has recently been reported for the patellar rotator cuff tendons (Millar et al., 2010). Mast cells contribute to the formation of scar/repair tissue in injured soft tissues (Kischer et al., 1978; Berton et al., 2000; Shiota et al., 2010), but surprisingly, their potential role in chronic tendon injury has been largely ignored. Using an experimentally validated acute tendon injury mouse model, it was found that mast cells play a role in influencing tendon repair, potentially by releasing TGF-beta at the site of injury (Sharma et al., 2011). The stimulus for increased mast cell number was not identified in the current study, and requires further work with suitable

laboratory models. Perhaps even more important is to determine whether inhibition of mast cell activation would influence the development or resolution of tissue pathology in response to tendon overuse.

In the process of neurogenic inflammation, SP binds to neurokinin 1 receptors (NK1R) on mast cells, causing them to release preformed substances contained in granules, as well as stimulating *de novo* leukotriene and prostaglandin production, mediating pain, edema, and fibrosis – common findings in chronically painful tendons despite the lack of "classical" (i.e., neutrophil- or macrophage-mediated) inflammation (Scott & Bahr, 2009). Gotoh and coworkers demonstrated a relationship between local SP levels measured via radioimmunoassay and the extent of shoulder pain in patients with rotator cuff tendinopathy (Gotoh et al., 1988). SP is expressed in small, peripheral sensory neurons in tendon as well as in tenocytes themselves (Backman et al., 2011), and its release can be triggered by noxious stimuli or by mechanical loading, respectively (Henry, 1976; Backman et al., 2011). As a potent neuropeptide and pain-producing substance, SP may be an important component to our understanding the basis of tendon pathology, and this point is emphasized by our current findings of increased mast cells – a likely target of SP in the tendinopathic tissue.

A significantly increased total intensity of PKB immunostaining was observed in the present study ($P = 0.03$). PKB is a key regulator of proliferation in many cell types, and has been shown to be activated (phosphorylated) in tenocytes in response to mechanical loading and to IGF-I, a key tendon mitogenic signal (Scott et al., 2007). In human tenocytes it has been shown that IL-1β induced PI-3K p85/PKB activation (Buhrmann et al., 2011). PKB activation has also been shown to potentiate TGF-beta-induced responses by phosphorylating negative regulators of TGF-beta signaling (Band et al., 2009). Further investigations are needed to outline the function of PKB in human tendinopathy and its potential impact on mast cell-derived TGF-beta signaling.

The rat Achilles tendinopathy treadmill model has previously been used with several variations to study activity-related tendon changes associated with mechanical loading (Glazebrook et al., 2008; Ng et al., 2011; Silva et al., 2011; Dirks et al., 2012). Glazebrook et al. coined the term "Rat-a-ped" to describe an uphill treadmill running model in which rats run for 1 h per day at 17 m/min. This model was reported to result in the development of morphological features consistent with early Achilles tendinopathy, including reduced collagen organization, evidence of increased vascularization, and increased tenocyte number. However, the published figures in the paper were difficult to interpret and appeared to display substantial levels of artifact, which did not appear to have been accounted for. In a subsequent paper, Scott et al. using the same protocol, reported morphological evidence of tenocyte rounding associated with pericellular collagen disorganization and increased glycosaminoglycan production which could indicate either an attempt to adapt, or a feature of very early, "reactive" tendinosis. Notably, neither of these papers actually quantified the extent of tendon pathology. Heinemeier et al. conducted the most extensive investigation of the Rat-a-ped model to date, and reported identical Bonar scores in control and Rat-a-ped rats, and no alteration in mechanical properties. This paper disproved the earlier interpretation of Scott et al. (BMC paper) that an observed, localized reduction in pericellular collagen organization in the Rat-a-ped model reflected a loss of collagen from the specimen. It is more likely that the organization of collagen fibrils rather than the amount of collagen is affected by loading in this model, given that Heinemeier demonstrated increased levels of type III collagen and reduced levels of type V collagen mRNA, and an improved biomechanical function in Rat-a-ped rats. The results of Heinemeier et al. would tend overall to refute the use of the Rat-a-ped model for studies of early tendinosis, but reinforce it as a model of *in vivo* tendon response.

In the present study, rats tolerated a larger volume of tendon loading than used in the Rat-a-ped model. Indeed, the overall level of work conducted by rats in the current study was similar to the Rat-a-ped model; however, it occurred over a 7-week, as opposed to a 16-week, period, representing therefore a substantial increase in the intensity of tendon loading. The corresponding changes in structure and cellularity in the tendon were quantified by the modified Bonar scale and found to be significantly increased. Although the overall Bonar scores were low and neurovascular proliferation typical of human lesions was absent, this model may be suitable for studying early *in vivo* load-induced responses. However, the validity of this model as a true model of overuse requires further validation, as certain key features of human pathology, particularly neovascularization but also more extensive glycosaminoglycan deposition, were not duplicated.

In the current study, the Bonar scores (intended to indicate the extent of tendon pathology by using a scale that has been well validated in human tendinopathy specimens) were relatively low. This finding is in contrast to a paper by Heinemeier et al. where normal rat tendons that were considered to be free of pathology were graded on average from 5 to 7.5 out of 15, depending on the region examined. In our study, the most common abnormality observed was tenocyte rounding (14 rats), increased cellularity (seven rats), and reduced collagen organization (seven rats). Increased vascularity was not observed in any tendon, and increased glycosaminoglycan staining was observed in only one tendon. The Bonar grading method may be limited at present in its utility due to lack of methodological

standardization. In particular, the question of which region to assess can cause considerable variation in scoring. In the current study, 10 tendons scored zero (no abnormality noted). The range of scores in tendons, which demonstrated abnormalities, was from 1 to 6. Future attention to the Bonar score would be useful to help in the standardization of scoring, as well as the validation of the score in rats and other species using defined injury stimulus known to lead to tendinopathic change (e.g., subfailure rupture or collagenase injection).

Because the Bonar scale relies on a subjective assessment of collagen organization, additional analysis of collagen structure using SHG analyses were made. The strength of SHG signal originating from histological sections taken from running rats was lower than that obtained from sedentary control rats ($P = 0.03$). This is in line with previous observations in the rat Achilles tendon showing a decrease of collagen organization after 12 weeks of mechanical loading (Abraham et al., 2011). The relative shift in collagen types seen with adaptation during uphill treadmill running in rats could also lead to a reduced SHG signal (Heinemeier paper), as an increase in type III collagen could lead to the formation of smaller collagen fibers.

An obvious but important limitation of this study is that it is observational rather than mechanistic. Although an association of increased mast cell density with tendon mechanical loading has been demonstrated, uncovering the mechanisms underlying this association will require further research.

In summary, the current study demonstrates that increased mast cell density is associated with calcaneal tendon structural changes that result from mechanical loading (7 weeks of uphill treadmill running). Mast cells may modulate the response of tendons to mechanical loading or injury.

Perspectives

The present study indicates that there might be a relationship between mast cells and early pathological changes in tendon tissue after overload. This study supports the theory that the early phase of tendinopathy is an inflammatory process, although not involving neutrophils in this instance. The problem of the late discovery of this injury is not solved with this knowledge; however, this study suggests that future research in diagnostic methods should continue to be addressed by an improved diagnosis of early inflammation, perhaps including mast cell activation, in tendon tissue that is being subjected to high volumes of mechanical loading.

Key words: tendinosis, exercise, collagen, rat.

Acknowledgements

We thank Damian Kayra for his great help and expertise in the SHGM analysis, and Julie Lorette and coworkers for excellent histological services.

References

Abate M, Silbernagel KG, Siljeholm C, Di Iorio A, De Amicis D, Salini V, Werner S, Paganelli R. Pathogenesis of tendinopathies: inflammation or degeneration? Arthritis Res Ther 2009: 11: 197–207.

Abraham T, Fong G, Scott A. Second harmonic generation analysis of early Achilles tendinosis in response to in vivo mechanical loading. BMC Musculoskelet Disord 2011: 12: 26.

Backman LJ, Fong G, Andersson G, Scott A, Danielson P. Substance P is a mechanoresponsive, autocrine regulator of human tenocyte proliferation. PLoS ONE 2011: 6: e27209.

Band AM, Bjorklund M, Laiho M. The phosphatidylinositol 3-kinase/Akt pathway regulates transforming growth factor-{beta} signaling by destabilizing ski and inducing Smad7. J Biol Chem 2009: 284: 35441–35449.

Berton A, Levi-Schaffer F, Emonard H, Garbuzenko E, Gillery P, Maquart FX. Activation of fibroblasts in collagen lattices by mast cell extract: a model of fibrosis. Clin Exp Allergy 2000: 30: 485–492.

Buhrmann C, Mobasheri A, Busch F, Aldinger C, Stahlmann R, Montaseri A, Shakibaei M. Curcumin modulates nuclear factor kappaB (NF-kappaB)-mediated inflammation in human tenocytes in vitro: role of the phosphatidylinositol 3-kinase/Akt pathway. J Biol Chem 2011: 286: 28556–28566.

Dirks RC. Fearon A, Scott A, Galley MR, Koch LG, Britton SL, Warden SJ. The effects of uphill treadmill running and collagenase on rodent Achilles tendons. In: Scott A, ed International Scientific Tendinopathy Symposium Vancouver. 2012.

Feng C, Beller EM, Bagga S, Boyce JA. Human mast cells express multiple EP receptors for prostaglandin E2 that differentially modulate activation responses. Blood 2006: 107: 3243–3250.

Glazebrook MA, Wright JR, Jr, Langman M, Stanish WD, Lee JM. Histological analysis of achilles tendons in an overuse rat model. J Orthop Res 2008: 26: 840–846.

Gotoh M, Hamada K, Yamakawa H, Inoue A, Fukuda H. Increased substance P in subacromial bursa and shoulder pain in rotator cuff diseases. J Orthop Res 1988: 16: 618–621.

Henry JL. Effects of substance P on functionally identified units in cat spinal cord. Brain Res 1976: 114: 439–451.

Khan KM, Cook JL, Kannus P, Maffulli N, Bonar SF. Time to abandon the "tendinitis" myth. BMJ 2002: 324: 626–627.

Kischer CW, Bunce H 3rd, Shetlah MR. Mast cell analyses in hypertrophic scars, hypertrophic scars treated with pressure and mature scars. J Invest Dermatol 1978: 70: 355–357.

Maffulli N, Wong J, Almekinders LC. Types and epidemiology of tendinopathy. Clin Sports Med 2003: 22: 675–692.

Millar NL, Hueber AJ, Reilly JH, Xu Y, Fazzi UG, Murrell GA, McInnes IB. Inflammation is present in early human tendinopathy. Am J Sports Med 2010: 38: 2085–2091.

Ng GY, Chung PY, Wang JS, Cheung RT. Enforced bipedal downhill running induces Achilles tendinosis in rats. Connect Tissue Res 2011: 52: 466–471.

Schmittgen TD, Livak KJ. Analyzing real-time PCR data by the comparative C(T) method. Nat Protoc 2008: 3: 1101–1108.

Scott A, Bahr R. Neuropeptides in tendinopathy. Front Biosci 2009: 14: 2203–2211.

Scott A, Cook JL, Hart DA, Walker DC, Duronio V, Khan KM. Tenocyte responses to mechanical loading in vivo: a role for local insulin-like growth factor 1 signaling in early tendinosis in rats. Arthritis Rheum 2007: 56: 871–881.

Scott A, Lian O, Bahr R, Hart DA, Duronio V, Khan KM. Increased mast cell numbers in human patellar tendinosis: correlation with symptom duration and vascular hyperplasia. Br J Sports Med 2008: 42: 753–757.

Sharma A, Abraham T, Sampaio A, Cowan M, Underhill M, Scott A. Sodium cromolyn reduces expression of CTGF, ADAMTS1, and TIMP3 and modulates post-injury patellar tendon morphology. J Orthop Res 2011: 29: 678–683.

Shiota N, Nishikori Y, Kakizoe E, Shimoura K, Niibayashi T, Shimbori C, Tanaka T, Okunishi H. Pathophysiological role of skin mast cells in wound healing after scald injury: study with mast cell-deficient W/W(V) mice. Int Arch Allergy Immunol 2010: 151: 80–88.

Silva RD, Glazebrook MA, Campos VC, Vasconcelos AC. Achilles tendinosis: a morphometrical study in a rat model. Int J Clin Exp Pathol 2011: 4: 683–691.

Theoharides TC, Alysandratos KD, Angelidou A, Delivanis DA, Sismanopoulos N, Zhang B, Asadi S, Vasiadi M, Weng Z, Miniati A, Kalogeromitros D. Mast cells and inflammation. Biochim Biophys Acta 2012: 1822: 21–33.